scientific reports

Check for updates

OPEN

# Individual-oocyte transcriptomic analysis shows that genotoxic chemotherapy depletes human primordial follicle reserve in vivo by triggering proapoptotic pathways without growth activation

S. Titus[1], K. J. Szymanska[1], B. Musul[1], V. Turan[1], E. Taylan[1], R. Garcia- Milian[2], S. Mehta[3] & K. Oktay[1]✉

**Gonadotoxic chemotherapeutics, such as cyclophosphamide, can cause early menopause and infertility in women. Earlier histological studies showed ovarian reserve depletion via severe DNA damage and apoptosis, but others suggested activation of PI3K/PTEN/Akt pathway and follicle 'burn-out' as a cause. Using a human ovarian xenograft model, we performed single-cell RNA-sequencing on laser-captured individual primordial follicle oocytes 12 h after a single cyclophosphamide injection to determine the mechanisms of acute follicle loss after gonadotoxic chemotherapy. RNA-sequencing showed 190 differentially expressed genes between the cyclophosphamide- and vehicle-exposed oocytes. Ingenuity Pathway Analysis predicted a significant decrease in the expression of anti-apoptotic pro-Akt *PECAM1* (p = 2.13E-09), *IKBKE* (p = 0.0001), and *ANGPT1* (p = 0.003), and reduced activation of PI3K/PTEN/Akt after cyclophosphamide. The qRT-PCR and immunostaining confirmed that in primordial follicle oocytes, cyclophosphamide did not change the expressions of *Akt* (p = 0.9), *rpS6* (p = 0.3), *Foxo3α* (p = 0.12) and anti-apoptotic *Bcl2* (p = 0.17), nor affect their phosphorylation status. There was significantly increased DNA damage by γH2AX (p = 0.0002) and apoptosis by active-caspase-3 (p = 0.0001) staining in the primordial follicles and no change in the growing follicles 12 h after chemotherapy. These data support that the mechanism of acute follicle loss by cyclophosphamide is via apoptosis, rather than growth activation of primordial follicle oocytes in the human ovary.**

In 2019, approximately 891,480 women were diagnosed with cancer in the U.S. alone, of whom 5.5% were in reproductive age[1], and potentially received fertility-damaging cancer treatments. Worldwide, chemotherapy-induced premature menopause and infertility are significant quality of life issues for young women diagnosed with cancer. To preserve fertility in the face of gonadotoxic chemotherapy, successful gamete, and gonadal tissue cryopreservation techniques have been developed[2]. However, these require at least minimally invasive procedures, and there have been no proven targeted medical treatments to block the ovarian damaging side effects of chemotherapy. If the mechanisms of chemotherapy-induced ovarian damage are understood, noninvasive, targeted pharmacological methods of fertility preservation can be developed.

Based on our earlier work, we suggest that chemotherapy causes both acute and delayed effects on the primordial follicle reserve. Chemotherapy agents such as doxorubicin, a topoisomerase inhibitor[3], and

[1]Department of Obstetrics, Gynecology and Reproductive Sciences, Yale University School of Medicine, New Haven, CT, USA. [2]Bioinformatics Support Program, Yale School of Medicine, New Haven, CT, USA. [3]Yale Center for Genome Analysis, Yale University, New Haven, CT, USA. ✉email: correspondence@fertilitypreservation.org

cyclophosphamide, an alkylating agent[4,5], cause apoptotic primordial follicle death by inducing DNA double-strand breaks (DSBs) in the human ovary. We found that the DNA damage peaks at around 12 h and subsequent follicle loss at 48 h, accounting for the acute loss of follicle reserve. Besides, we also showed in in vivo human ovarian xenograft models that doxorubicin causes stromal cell death as well as microvascular damage, inducing tissue hypoxia, which may contribute to the delayed loss of ovarian follicles. Others have also shown possible stromal damaging effects of cancer drugs in women[6]. It has also been proposed in rodent models that cyclophosphamide may induce depletion of primordial follicle reserve via inducing a massive entry of follicles into the growth phase[7]. It was surmised that this follicle 'burn-out' is the acute result of the direct activation of phosphoinositide 3-kinase/phosphatase and tensin homolog/protein kinase B (PI3K/PTEN/Akt) pathways, which regulate primordial follicle growth initiation. There could be several reasons for these discrepancies, including the possibility of the differing mechanism being in play at acute and delayed phases after the chemotherapy exposure[8]. Moreover, in vitro or rodent models may not be representative of in vivo changes in human ovary responses to chemotherapy. Therefore, mechanistic studies are needed to delineate the acute impact of chemotherapy on ovarian follicle reserve. Utilizing a human ovarian xenografting coupled with laser-capture-microdissection-assisted individual-oocyte RNA-sequencing (RNA-seq) and quantitative real-time PCR (qRT-PCR) approaches perfected by our team, we performed the first human in vivo single-cell transcriptomics study to determine the molecular mechanisms of acute chemotherapy-induced loss of primordial follicles in the human ovary[4,5].

## Materials and methods

**Mice.** Female severe combined immunodeficiency (NOD-SCID) mice aged 2–3 months were obtained from Taconic farms and housed under pathogen-free conditions. Animals were kept in a 12 h light–dark cycle and provided ad libitum with water and a laboratory diet. All animal experiments were approved and conducted in accordance with Yale University's animal research requirements, using protocols approved by the Institutional Animal Care and Use Committee.

**Ovarian xenografts.** Ovarian cortical pieces from four cadaveric organ donors aged ≤ 32 years were cryopreserved according to our established protocol[9,10]. Tissue pieces 2–3 $mm^3$ (2–3 × 1 × 1 mm) were xenografted subcutaneously to SCID mice, as described previously[4]. Briefly, after animals were anesthetized, a small incision was made on the dorsal midline of the animal. Human ovarian cortex fragments from four different donors were transplanted to each animal (n = 4 tissue pieces/animal). The grafts were distributed in a way that a sample from each different donor was present in each condition. After allowing xenografts to fully vascularize for 10 days, the mice were given a single intraperitoneal (i.p.) dose of cyclophosphamide (75 mg/kg) or the vehicle. The tissues were then recovered 12 h later and prepared for either histology and immunohistochemistry or embedded in a medium for frozen sectioning and isolation of primordial follicle oocytes by laser capture dissection microscopy.

All methods were carried out in accordance with relevant guidelines and regulations consistent with the Declaration of Helsinki. The utility of human ovarian tissue was exempted by the Yale Institutional Review Board as the tissues are from deceased, non-living cadavers. Research on deceased organ donor cadaver tissue is not considered human subjects research and is exempt from IRB oversight. However, the LiveonNY scientific board reviewed and approved our study protocol and consent was obtained from the relatives of deceased organ donors to donate ovarian tissue to research, along with other organs for transplant procedures.

**Immunohistochemistry.** Ovarian tissues were fixed in 4% paraformaldehyde (PFA), embedded in paraffin, and serially sectioned at 5-micron intervals. Sections were stained with Hematoxylin and Eosin (H&E) for differential follicle counts, as previously described[4]. Every fifth section of an entire xenograft was chosen for staining (7–8 stained slides from a total of 30–35 slides per xenograft) and evaluated by observers who were blinded to the intervention and each other's findings. To avoid over-counting, follicles were recorded only when the nucleus was visible. Follicles were classified based on our previously established criteria[11]. A primordial follicle was defined as an oocyte surrounded by a single layer of flattened, squamous follicular cells. A primary follicle was defined as an oocyte surrounded by a single layer of cuboidal granulosa cells. A follicle was classified atretic based on morphological criteria, including nuclear pyknosis, cytoplasm contraction, and nuclear pyknosis of granulosa cells and dissociation of the granulosa cells from the basal membrane[12,13].

Randomly selected sections coming from ovarian tissue of least 3 different individuals were used for immunohistochemistry for Anti-active Caspase-3 (AC-3, 1:1000, AF-835, R&D Systems), γH2AX (1:250 IHC-00059, Bethyl Laboratories), rabbit phospho-Akt (S473, 1:400, #4060S, Cell Signaling Technology, Denver, MA), rabbit phospho-rpS6 (S235-236, 1:100; #2211S, Cell Signaling Technology, Denver, MA), and phospho-FOXO3A (S253, 1 µg/ml, # ab47285, Abcam, Cambridge, MA, USA)[3]. Images were captured on an Olympus IX73 microscope. For double immunofluorescent staining, the slides were deparaffinized, subjected to heat-induced antigen retrieval with citrate buffer and subsequently blocked with 1% BSA and 5% normal goat serum. The mix of primary antibodies BAD (1:250, A302-384A, Bethyl Laboratories) and Bcl2 (1:200, sc-509, Santa Cruz Biotechnology) was used. The secondary antibodies were conjugated with Alexa 488 (1:500, A11001, Invitrogen) and Alexa 594 (1:500, A11012, Invitrogen). The slides were counterstained with DAPI (1 µg/ml, D3571, Invitrogen), and mounted with ProLong Gold (P36930, Life Technologies). The imaging and intensity calculations were done on Nikon 90i Eclipse microscope. By overlapping both BAD and Bcl2 staining color channels, and selecting the area around primordial follicles, we calculated the mean pixel intensities. We compared the intensity means between primordial follicle oocytes of vehicle and chemo groups after subtracting the background, which was set based on the negative control, and by setting a constant threshold for both channels across the images. Stringent experimental conditions ensured that the threshold values did not change significantly from day to day of image acquisition. For the calculation, we used 3 slides of each xenografted tissue, and 'n' represents the number

of different tissue pieces. The analysis was done using ImageJ software. Additional representative images were acquired on a Leica SP8 Gated STED 3X Super Resolution confocal microscope using 60 × oil immersion lens.

**Laser-capture microdissection (LCM) and isolation of single primordial follicle oocytes.** After harvesting ovarian xenografts, tissue blocks were immediately prepared in optimum cutting temperature (OCT) compound and stored at − 80 °C until cryostat sectioning (− 20 °C). These were later sectioned at 8-micron thickness and stained with H&E according to the manufacturer's protocol. Based on the morphological appearance, i.e., follicle with a single layer of flat granulosa cells around with positively stained oocyte inside, single primordial follicle oocytes were individually isolated using an LCM excluding any pre-granulosa cell from the dissection (see Supplementary Video S1). LCM was performed on the Leica LMD7000 microscope, under 40 × magnification. To each Eppendorf tube, filled with cell lysis buffer (RNase inhibitor in 0.2% (vol/vol) Triton X-100 solution), the individual primordial oocyte was collected from 2–3 adjacent tissue sections to ensure that one full cell was included (Leica Microsystems, Buffalo Grove, IL, USA).

**RNA-seq analysis on laser captured single primordial follicle oocytes.** The primordial follicle oocytes were processed for sequencing with modifications of a previously established protocol on non-germline single cells for LCM material[14]. Samples were sequenced to depths of up to 44 million read pairs, 75 nt length reads per sample using the Illumina Rapid v2 kit (75 cycles) on an Illumina HiSeq2500 Sequencing System. Image analysis, base calling, and generation of sequence reads were produced using the HiSeq Control Software v2.0 (NCS) and Real-Time Analysis Software (RTA). Data were converted to FASTQ files using the bcl2fastq2 v1.8.4 software (Illumina Inc.). The reads were trimmed for quality. Those were then aligned to the human reference genome (hg38 gencode for humans) using HiSAT2[15]. The alignments were processed using Ballgown (free online software)[15], and per-gene counts were obtained. The raw counts were processed using DESeq2 and R.

**Gene network and pathway analysis.** Ingenuity Pathway Analysis (IPA) Ingenuity Systems QIAGEN, Content version: 45865156, 2018, Redwood City, CA, USA) was used to carry out pathway analysis for differentially expressed genes across samples. Each gene symbol was mapped to its corresponding gene object in the Ingenuity Pathways Knowledge Base. The over-represented pathways are ranked according to the calculated *Benjamini–Hochberg* FDR $P < 0.05$[16].

**qRT-PCR on laser captured primordial follicle oocytes.** RNA from single primordial follicles was amplified, and cDNA was prepared using established protocol[14], and gene expression analysis was done by qRT-PCR using Syber Green (Applied Biosystems Warrington, UK) on ABI QuantStudio-6 Flex Real-Time PCR machine. PCR cycling conditions were 95 °C for 5 min and 45 cycles of 10 s at 95 °C, 58 °C for 15 s, and 72 °C for 15 s, followed by a melting curve analysis to confirm the single, specific products. The expression level of each mRNA was calculated by the comparative Ct method (ΔΔCt), and the fold change (FC) was calculated by the Eq. $2^{-\Delta\Delta Ct}$. β-Actin was used as a reference gene for normalization. Primers for qRT-PCR reactions are specified in Supplementary Table S1 and were obtained from IDT (USA). 'n' indicates the number of single follicles. Each experiment contained primordial follicles from at least 3 different tissue donors.

**Statistics.** For RNA-seq analysis, we determined statistical significance for differential gene expression based on the q-value (or the False Discovery Rate), with stringent cut-offs of 0.05 or less. This ensures that the Type II error is kept as low as possible, given the constraints of sample size. Our observations of gene transcript abundances by RNA-seq from a relatively low sample-size are justified as we observe similar trends while interrogating the samples using other more direct biological and biochemical approaches such as qRT-PCR analysis and immunohistochemistry. Other data from chemotherapy- and vehicle-treated groups were compared using Student's two-tailed t-test. P values less than 0.05 were considered significant. For statistical analysis we used GraphPad Prism 6 (GraphPad Software, San Diego, CA).

## Results

**Cyclophosphamide treatment does not increase primordial follicle growth initiation in vivo; it induces DNA DSBs and apoptotic death.** First, to morphologically determine if cyclophosphamide exposure increases the entry of primordial follicles into the growth pool, we calculated the ratio of primary to primordial follicles (py/pd = follicle growth initiation index) in xenografts[17]. Based on the growth initiation ratio, we are only able to give an estimate, and not a definite answer of the follicle fate since we use only a small fragment of the cortex and of the unequal distribution of the follicles in each tissue. For H&E and AC-3 staining, we analyzed a total of 70 follicles (51 primordial and 19 primaries) from 3 slides of 8 different tissue pieces for the vehicle group and 202 follicles (177 primordial and 25 primaries) from 3 slides of 10 pieces of cortex from the chemo-treated group. We found no significant difference in the py/pd ratio between the vehicle and the cyclophosphamide -treated group (34.62 ± 7.94, vs. 19.97 ± 6.79; $p = 0.17$) (Fig. 1A). Because atretic follicles may not initiate growth, we also analyzed the ratio of non-atretic py/pd follicles. We, again, did not observe a significant difference in follicle growth initiation rate between the vehicle- and cyclophosphamide-treated groups (34.59 ± 9.75 vs. 18.58 ± 10.21; $p = 0.08$) (Fig. 1B).

Next, we studied whether cyclophosphamide induces apoptotic oocyte death using AC-3 immunostaining. We found a significant increase in the percentage of apoptotic primordial (65.03% ± 3.55% vs. 28.27% ± 5.77%; $p < 0.0001$ cyclophosphamide vs vehicle) and primary follicles (63.67% ± 9.89%, $n = 8$ vs. 28.57% ± 8.74%; $n = 10$; $p = 0.01$ cyclophosphamide vs vehicle) indicating that cyclophosphamide caused massive apoptotic follicle death

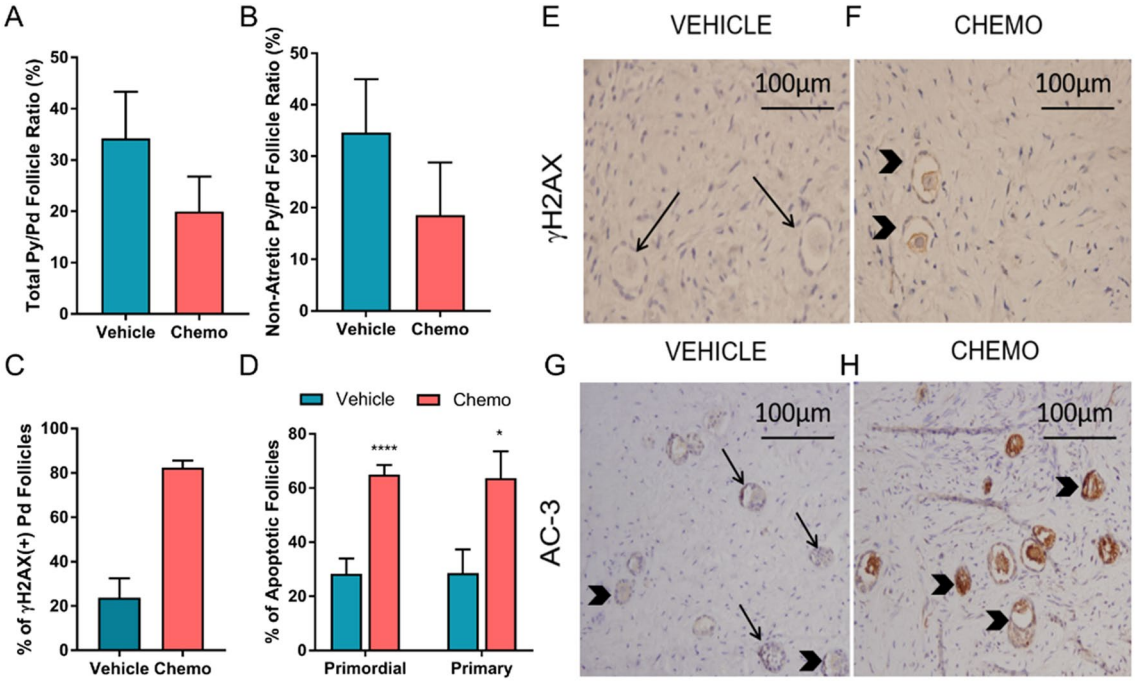


**Figure 1.** Cyclophosphamide does not trigger follicle growth initiation in vivo but induces DNA DSBs and apoptosis in human primordial follicles 12 h after exposure. There was no significant difference observed in (**A**) total ($p = 0.17$), (**B**) non-atretic ($p = 0.08$) primordial follicle growth initiation rate as calculated by primary to primordial (py/pd) follicle ratios ($n_{vehicle} = 8$, $n_{chemo} = 10$). (**C**) Chemotherapy treatment induced significant DNA damage (γH2AX positive+) in primordial follicles ($p = 0.0001$). (**D**) There was a significant increase in the percentage of apoptotic primordial ($p = 0.001$) and primary ($p = 0.01$) follicles in cyclophosphamide -treated samples ($n_{vehicle} = 8$, $n_{chemo} = 10$). Photomicrographs of γH2AX (**E**,**F**) and AC-3 staining (**G**,**H**) positive follicles in vehicle- and cyclophosphamide -treated (chemo) groups. Black arrows indicate negative, black arrowheads show follicles positive for AC-3 and γH2AX. The 'n' equals the number of xenografted ovarian tissue, data are presented as mean ± S.E.M.

within 12 h of treatment (Fig. 1D,G,H). Moreover, confirming earlier reports, we found by γH2AX staining that chemotherapy induced DNA DSBs in primordial follicles compared to the vehicle treatment (82% ± 3.1%, n = 58 individual oocytes captured from 10 xenografts vs. 23.82% ± 8.66%, n = 24 individual oocytes captured from 8 xenografts; $p = 0.0002$) (Fig. 1C,E,F).

**Individual-oocyte RNA-seq analysis of pathways activated in primordial follicles in acute response to chemotherapy in vivo.** We performed high throughput RNA-seq on non-atretic, individual primordial follicle oocytes from cyclophosphamide—and vehicle-treated xenografts to have a broader view of the pathways that are altered in primordial follicles in acute response to chemotherapy. For each condition, we used two individual primordial follicles from each of the two different donor ovaries. On average, 29.8 mln reads were obtained per sample with 74% alignment to the human genome. To verify that the obtained material represents oocyte transcriptome, the expression of oocyte-specific genes, such as ZP3, KIT and DDX4 was confirmed in all the samples. We found that 190 genes were differentially expressed between the chemo- and vehicle-treated groups (fold change ≥ 2, $p < 0.05$) (Fig. 2A and Supplementary Table S2). We then performed IPA enrichment analysis (Qiagen) to determine significantly altered (Fig. 2B) canonical pathways ($p = 0.05$; fold change [fc] = 2). We found that with chemo-exposure, the Fcγ Receptor-mediated Phagocytosis in Macrophages and Monocytes ($p = 0.005$), Phospholipase C Signaling ($p = 0.005$), Ephrin Receptor Signaling ($p = 0.005$) and Interleukin-8 signaling ($p = 0.03$) were suppressed. We also found significant changes in Axonal Guidance Signaling ($p = 0.0003$), Gap junction signaling ($p = 0.01$), and Focal Adhesion Kinase (FAK) Signaling ($p = 0.04$), but no predictions could be made as to the direction of change. The Phospholipase C Signaling, Ephrin Receptor Signaling, and IL8 signaling pathways are known to be associated with inhibition of apoptosis. We used IPA to generate the network connecting the genes present in these pathways with the apoptosis function ($p = 5.37E{-}19$) and to predict if apoptosis is favored based on the expression status of these genes in our data. The IPA suggested activation of apoptotic processes in the chemotherapy-treated samples (Supplementary Fig. S1). Further, we used IPA to find the overlap between the differentially expressed genes after chemotherapy exposure and those genes in the IPA knowledge base associated with the functions of apoptosis and activation of primordial follicles. We found in our data set that *PTEN, Akt-1 Foxo3, BAD, ANGPT1, Pde* and *BTG2* overlapped with apoptotic function ($p = 3.58E{-}18$), while *PTEN* and *KITLG* overlapped with the activation function of ovarian follicles ($p = 7.90E{-}07$). The analysis of our dataset showed that the growth activation of the primordial follicle is inhibited while apoptosis is triggered in acute response to chemotherapy in vivo (Fig. 2C).

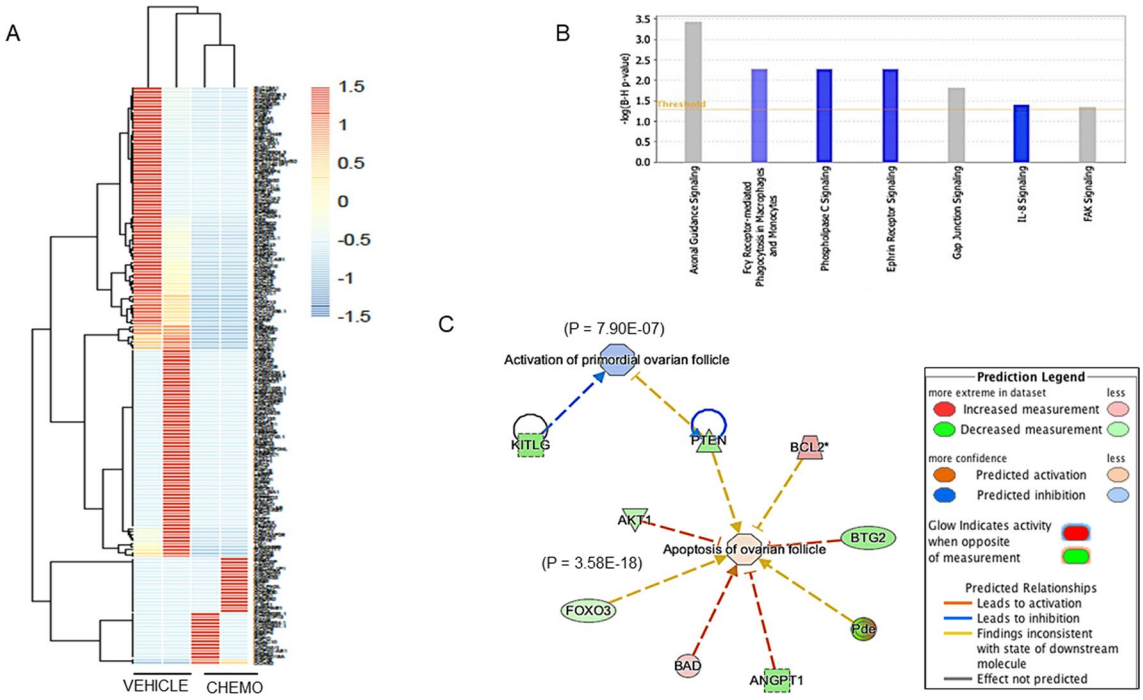


**Figure 2.** Individual-oocyte RNA-Sequencing and Ingenuity Pathway Analysis (IPA) Results. (**A**) Heat map of genes that are significantly altered 12 h after cyclophosphamide exposure compared to the vehicle treatment. The pheatmap package in R software was used for visualization. (**B**) Major pathways that were found to be significantly altered after chemotherapy exposure. The over-represented pathways are ranked according to the calculated *Benjamini–Hochberg* FDR, $p < 0.05$. (**C**) IPA was utilized to find the overlap between the differentially expressed genes in our study and those genes in the IPA knowledge base associated with the functions of apoptosis and activation of primordial follicles. This analysis predicted relationships that favored apoptosis and inhibition of the Akt pathway in primordial follicles 12 h after chemotherapy exposure.

Supporting these findings, RNA-seq analysis showed that cyclophosphamide did not cause transcriptomic activation PI3K/PTEN/Akt pathway genes, which are responsible for primordial follicle growth initiation. Specifically, RNA-seq analysis showed a significant decrease in the expressions of *PECAM1* ($p = 2.13E-09$), *IKBKE* ($p = 0.001$) and *ANGPT1* ($p = 0.03$) (Fig. 3A–C) in the cyclophosphamide -treated samples when compared to the vehicle. These genes have anti-apoptotic functions and are also known activators of Akt[18–22]. Further analysis of the PI3K/PTEN/Akt pathway in the cyclophosphamide-treated samples showed a trend toward a decline in *Akt-1* ($p = 0.19$) and no significant change in the expressions of *Foxo3a* ($p = 0.8$) and *rpS6* ($p = 0.36$) (Fig. 3D–F). These findings suggest that cyclophosphamide treatment does not result in the activation of follicle growth or anti-apoptotic pathways but triggers an acute apoptotic response.

**qRT-PCR and immunohistochemical confirmation of chemotherapy-induced acute pathway changes in human primordial follicles.** To further explore and confirm the expression patterns of the PI3K/PTEN/Akt pathway members in primordial follicle oocytes in acute response to chemotherapy, we performed qRT-PCR analysis on LCM, individual primordial follicle oocytes. Based on the relative gene expression analysis, we found no change in the expressions of *Akt-1* ($n_{vehicle} = 5$ and $n_{chemo} = 6$; $p = 0.93$), *rpS6* ($n_{vehicle} = 5$ and $n_{chemo} = 6$; $p = 0.32$) and *Foxo3a* expression ($n_{vehicle} = 5$ and $n_{chemo} = 6$; $p = 0.12$) 12 h after cyclophosphamide exposure compared to the vehicle (Fig. 4A). To further confirm our findings, we investigated the changes in the immunohistochemical expression of the key PI3K/PTEN/Akt pathway proteins in response to chemotherapy (Fig. 4B). We calculated the percentage of positive to the total number of follicles from 3 slides per xenografted tissue, 'N' indicating the number of primordial follicles analyzed, 'n' indicating the number of xenografts from which the follicles originated. We observed no significant differences between the vehicle and cyclophosphamide treatment groups in the expressions of p(phospho)-Akt ($7.29 \pm 0.22$, $N = 58$, $n = 8$ vs. $11.59 \pm 0.8$, $N = 149$, $n = 6$; $p = 0.52$), p-Foxo3a ($12.03 \pm 1.48$, $N = 38$, $n = 9$ vs. $18.85 \pm 1.43$, $N = 162$, $n = 8$; $p = 0.63$), and p-rpS6 ($6.06 \pm 0.14$, $N = 38$, $n = 11$ vs.$12.55 \pm 0.94$, $N = 114$, $n = 7$; $p = 0.4$). These results further confirm that chemotherapy does not activate the PI3K/PTEN/Akt pathway in primordial follicles within 12 h of exposure.

**Chemotherapy activates pro-apoptotic BAD-Bcl2 action.** *Bcl2* (B-cell lymphoma 2) is a known anti-apoptotic gene[23]. It is localized to the outer membrane of the mitochondria, and it plays an important role in promoting cell survival via inhibiting the actions of pro-apoptotic genes such as the *BAD*. By qRT-PCR analysis of laser-captured primordial follicle oocyte we observed a trend towards declining expression of *Bcl2* ($n_{vehicle} = 5$ and $n_{chemo} = 6$; $p = 0.17$), but together with *BAD* ($n_{vehicle} = 5$ and $n_{chemo} = 6$; $p = 0.93$), it did not reach statistical significance in the cyclophosphamide -treated xenografts vs. the vehicles (Fig. 5A,B). Certain stress conditions,

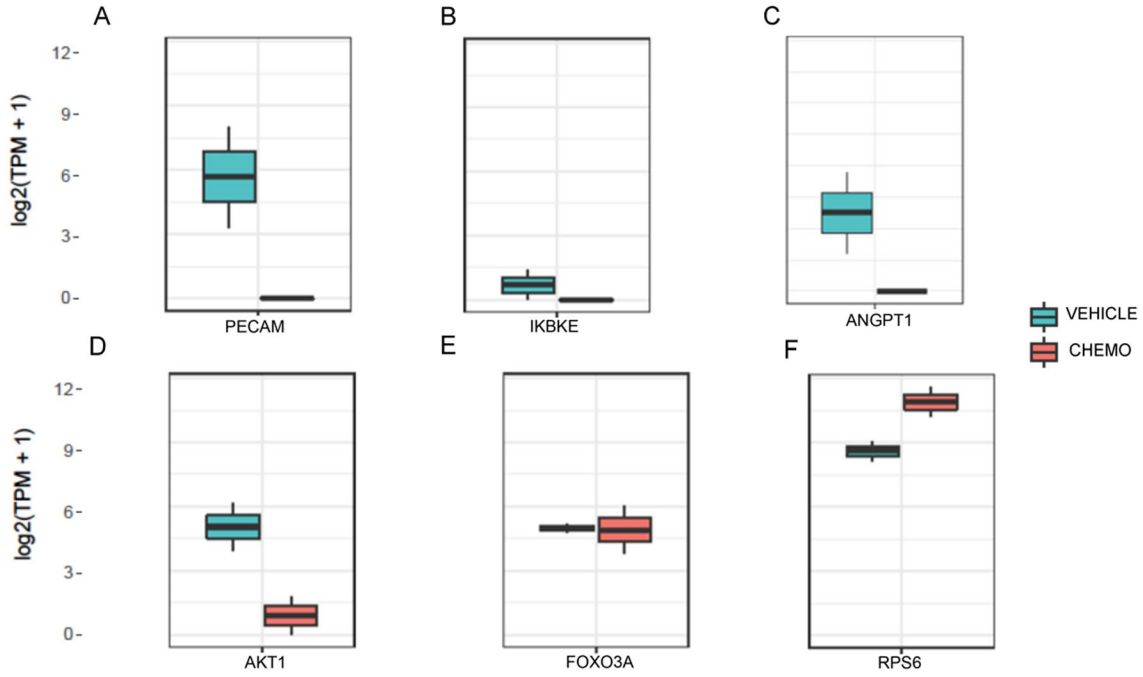


**Figure 3.** RNA-Sequencing results indicating lack of activation of the PI3K/PTEN/Akt pathway in vivo 12 h after chemotherapy exposure. Significant decrease in the expression of (**A**) *PECAM1* (p = 2.13E−09), (**B**) *IKBKE* (p = 0.001) and (**C**) *ANGPT1* (p = 0.03) that are reported to be anti-apoptotic with pro effects on the PI3K/PTEN/Akt pathway. In cyclophosphamide-treated samples, there was a trend towards a decline in the expression of PI3K/PTEN/Akt pathway member *Akt-1* (p = 0.19) (**D**) while no changes in the expressions of the *Foxo3a* (p = 0.8) (**E**) or *rpS6* (p = 0.36) (**F**) were observed. R software was used to generate the image.

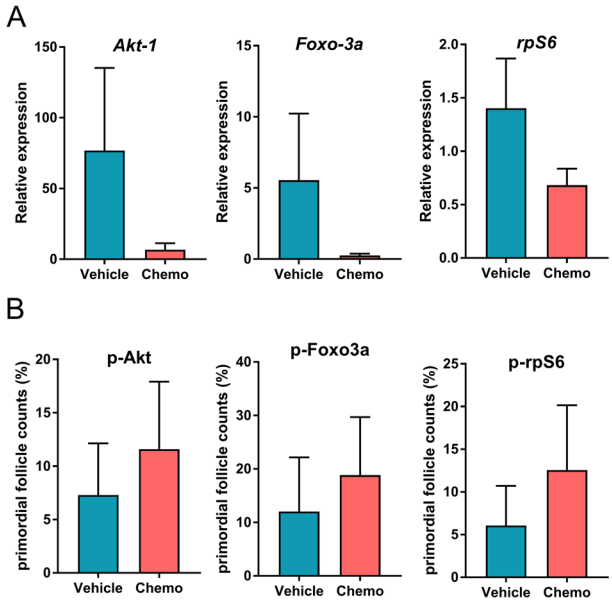


**Figure 4.** Validation of individual primordial follicle oocyte RNA-seq results by qRT-PCR and immunochemistry. (**A**) qRT-PCR analysis of PI3K/PTEN/Akt pathway genes shows no significant change in the expression of Akt-1 ($n_{vehicle} = 5$ and $n_{chemo} = 6$; p = 0.93), rPS6 ($n_{vehicle} = 5$ and $n_{chemo} = 6$; p = 0.32) or Foxo3a ($n_{vehicle} = 5$ and $n_{chemo} = 6$; p = 0.12) in the cyclophosphamide-treated group (chemo) as compared to the vehicle. The 'n' indicates the number of single primordial follicles analyzed, data are presented as mean of the ΔΔCt ± S.E.M. (**B**) There is no change in the percentage of primordial follicles stained for (phospho)-Akt (7.29 ± 0.22, n = 8 vs. 11.59 ± 0.8, n = 6; p = 0.52), p-Foxo3a (12.03 ± 1.48, n = 9 vs. 18.85 ± 1.43, n = 8 ; p = 0.63), and p-rpS6 (6.06 ± 0.14, n = 11 vs.12.55 ± 0.94, n = 7; p = 0.4) after cyclophosphamide treatment. The 'n' indicates the number of xenografted ovarian cortex tissues, data are presented as mean ± S.E.M.

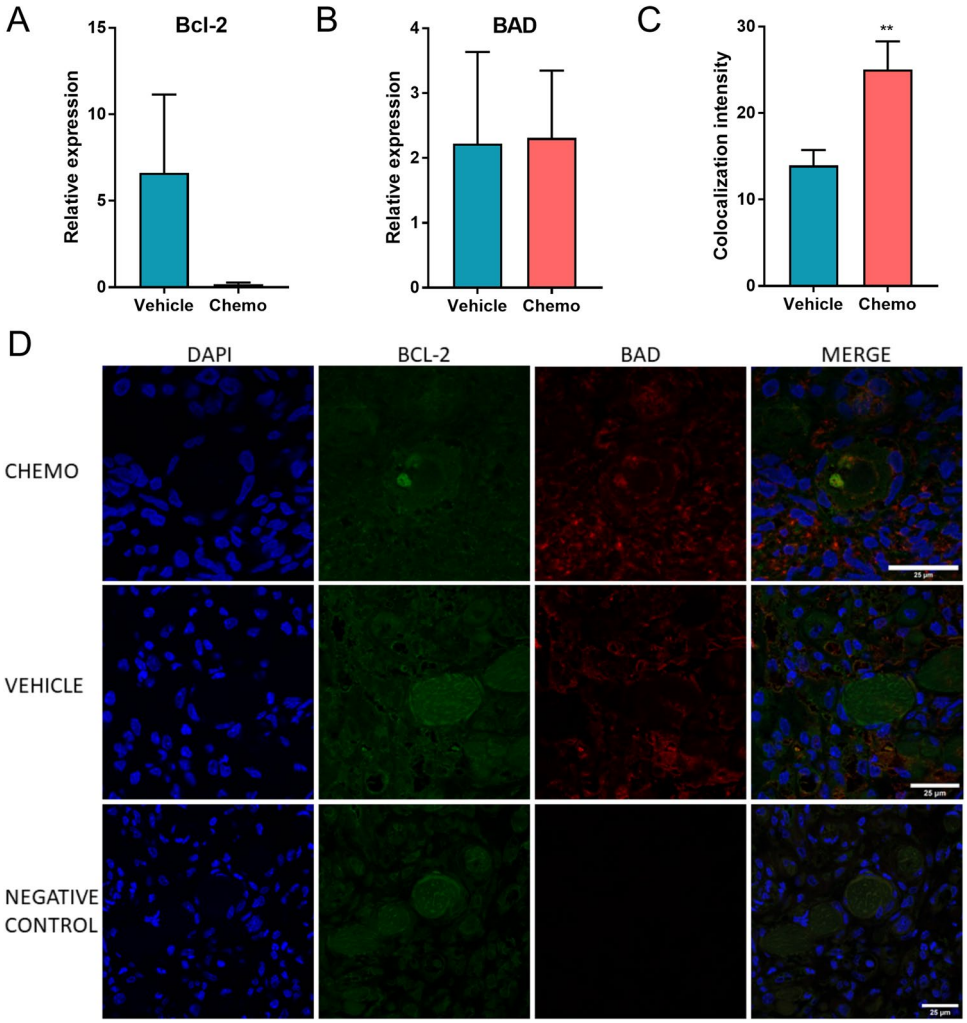


**Figure 5.** qRT-PCR and immunostaining analysis of BAD-BCL2 12 h after cyclophosphamide exposure. qRT-PCR analysis shows no significant change in the expression of both (**A**) Bcl-2 ($n_{vehicle} = 5$ and $n_{chemo} = 6$; $p = 0.17$) and (**B**) BAD ($n_{vehicle} = 5$ and $n_{chemo} = 6$; $p = 0.93$) after cyclophosphamide exposure (chemo) compared to the vehicle group. The 'n' indicates the number of single primordial follicle oocytes analyzed, data are presented as ΔΔCt mean of the ± S.E.M. (**C**) By Image J analysis, the BAD-BCL2 colocalization intensity was increased in primordial follicles after cyclophosphamide exposure ($n = 6–7$; $p = 0.004$), 'n' indicates the number of different xenografted tissue pieces, data are presented as mean ± S.E.M. (**D**) Confocal images representative of BAD-BCL2 staining in the primordial follicles showing the chemo-treated, vehicle, and negative control samples. Blue represents nuclear DAPI staining, BCL-2 and BAD are shown in green and red, respectively. Images were obtained using 60 × magnification, oil immersion lens on Leica SP8 Gated STED 3X Super Resolution confocal microscope. Scale bar = 25 µm.

such as oxidative stress and DNA damage, initiate the Bcl-2 protein family—related apoptotic response[24–26]. BAD is activated by dephosphorylation and dimerizes with BCL2, preventing it from its anti-apoptotic function, and promote apoptosis[27,28]. Therefore, we studied the BAD-Bcl-2 colocalization in response to chemotherapy. We showed a significantly increased colocalization of BAD and BCL2 protein staining in cyclophosphamide-treated samples ($N = 18$, $n = 6$) compared with the vehicle ($N = 20$, $n = 7$; $p = 0.004$) (Fig. 5C,D), which may suggest increased protein colocalization and potential interactions. 'N' indicating the number of primordial follicles analyzed, 'n' indicating the number of xenografts from which the follicles originated. These results collectively indicate that within 12 h, chemotherapy exposure results in increased liability to apoptotic death in primordial follicle oocytes, possibly via the BAD-Bcl2 pathway.

## Discussion

Maintenance of primordial follicle reserve is crucial for the reproductive life span of a female individual. This reserve incurs a massive loss when a patient undergoes chemotherapy treatment, later presenting itself as early menopause and infertility. In this study, we demonstrated the molecular mechanisms of chemotherapy-induced acute damage to ovarian primordial follicles using our unique in vivo human ovarian xenograft model and single-cell transcriptomic approaches. Because our earlier work showed that human primordial follicle apoptosis peaks

12 h post-exposure to chemotherapy[5], and as our focus was to determine the mechanisms of acute follicle loss after cancer treatments, we limited our experiments to 12 h time point. We provided multiple lines of evidence converging that cyclophosphamide induces primordial follicle death by prompt activation of apoptotic death pathways, not the PI3K/PTEN/Akt pathway. While we showed that within 12 h of treatment, chemotherapy induces DNA DSBs in human oocytes, we found no evidence that it results in increased growth activation of primordial follicles. Likewise, our previous immunohistochemical analyses in rodents and human ovarian xenograft models showed that both cyclophosphamide and doxorubicin induce DSBs and apoptotic oocyte death in primordial follicles[3].

In this unique in vivo human ovarian xenograft model, we first showed that chemotherapy exposure did not acutely result in the change of total and non-atretic primary vs. primordial follicle ratio rather, it induced DNA DSBs and AC-3 expression in primordial follicles. This morphological evidence supports that chemotherapy induces primordial follicle apoptotic death rather than growth initiation (Supplementary Fig. S2).

The morphological data was then backed by LCM-based individual-oocyte RNA-seq and IPA analysis, which we used to interrogate the key pathways that are activated in primordial follicles in response to chemotherapy. The LCM-based cell isolation method enables us to precisely capture individual primordial follicle oocytes from ovarian tissue where they are identified based on their morphology without the need of unique genetic markers (Supplementary Video S1). This initial screening directed us towards pathways related to apoptotic processes rather than those that are involved in follicle growth activation as culprits in acute chemotherapy-induced ovarian reserve loss. Considering that the number of the sequenced primordial oocyte follicles was relatively small, we then confirmed these findings by qRT-PCR and immunohistochemistry in a larger number of samples (n = 5–6 and n = 8–11, where 'n' is the number of single primordial follicle oocytes and number of xenografted ovarian tissues belonging to different donors, respectively).

The transcriptomic analysis with our LCM-based individual-oocyte RNA-sequencing approach indicated suppression of several signaling pathways such as Phospholipase-C (PLC), Ephrin (Eph) Receptor, and IL-8 that are anti-apoptotic and involved with Bad-Bcl2-mediated apoptosis[29–31]. Activation of IKBKE induces NF-κB nuclear accumulation and DNA-binding activity by phosphorylation, which then increases the transcription of *BCL2*[32]. Although we did not find a significant decrease in the expression of pro-survival gene BCL-2 and pro-apoptotic BAD, we observed an increased colocalization of BAD with BCL2, which indicates an increased tendency for apoptotic death in human primordial follicle oocytes. We, on the other hand, did not find an increase in the phosphorylation of the key PI3K/PTEN/Akt members in acute response to chemotherapy. Though the follicle growth activation via PI3K/PTEN/Akt pathway is primarily regulated by protein phosphorylation, a previous study suggested that the inducible ablation of Foxo3a was associated with primordial follicle depletion through growth activation[33]. Therefore, we additionally studied transcriptional changes in individual primordial follicle oocytes by qRT-PCR and also did not find a change in response to chemotherapy exposure. These converging findings support the common theme that chemotherapy induces human primordial follicle death via apoptotic pathways rather than massive follicle growth activation and resulting 'burn-out' in the acute phase. While our data cannot rule out the activation of the primordial follicles at the later time point, it confirms apoptosis as the acute response of the oocyte to chemotherapy.

In agreement with our findings in humans, other studies in rodents showed that alkylating agents busulfan and cyclophosphamide induce apoptosis and deplete primordial follicle reserve[8,34–37]. Studies in mouse oocytes also showed that cyclophosphamide induces a reduction in mitochondrial transmembrane potential and accumulation of cytochrome-c in the cytosol, leading to activation of the caspase family and apoptosis[38]. A plethora of factors such as DNA damage, energy stress, loss of growth factor signaling and hypoxia can trigger apoptosis by activation of BCl2 pathway proteins[39]. In our previous in vitro and xenografting studies, we showed that a topoisomerase inhibitor, cancer drug doxorubicin induces DNA DSBs and apoptosis in primordial follicles[3]. In this study, cyclophosphamide treatment likewise increased DNA DSBs, as shown by increased expression of γH2AX staining in the primordial follicles. Increased DNA damage in primordial follicles is a likely stress signal for the recruitment of the pro-apoptotic BCL2 that causes the activation of the apoptotic cascade in the primordial follicles.

Our individual-oocyte transcriptomic analyses also showed significant downregulation of platelet endothelial cell adhesion molecule-1 (PECAM), and Angiopoietin-1(ANGPT1) (Fig. 3D–F). Previous studies have shown that Jurkat cells with a 70% reduction of PECAM-1 expression by siRNA-silencing were significantly more sensitive to chemotherapy-induced apoptosis[40]. Neuronal cell death was caused by the downregulation of Ang-1 (a.k.a. ANGPT1, followed by Akt pathway inhibition[41]. It is also shown that Ang-1 induces phosphorylation of Akt, which is associated with the up-regulation of the apoptosis inhibitor survivin[22]. Inhibition of ANGPT1 in rat follicles increased the levels of AC-3 and decreased Akt phosphorylation[41]. The latter concurs with our finding of increased AC-3 expression after chemo exposure in primordial follicles and brings up the interesting possibility that chemo exposure may indeed result in the suppression of Akt functions, which further favors apoptosis. Interestingly, in addition to PECAM and ANGPT1, IKBKE is also a positive regulator of Akt activation[19,21,22], which we found to have decreased in expression in primordial follicles after chemotherapy.

In summary, our novel in vivo single-cell human transcriptomics data show that by suppression of anti-apoptotic mechanisms, gonadotoxic chemotherapy exposure induces a pro-apoptotic state in primordial follicles in the acute phase (Fig. 6). Rather than PI3K/PTEN/Akt pathway activation resulting in massive follicle growth and 'burn-out', we found contrary evidence that chemotherapy may favor inactivation of the pathway. Nonetheless, our study only focused on the acute effects of chemotherapy, and we chose the 12 h timepoint based on our earlier xenograft work[5]. It is likely that the apoptotic process was well underway by the 12th hour time point, and future studies may be needed to dissect the timeline of earlier events. It is also possible that further follicle loss occurs at later time points as a result of additional mechanisms such as the stromal/microvascular damage and follicle activation[8] and the potential delayed mechanisms of chemotherapy-induced ovarian reserve loss should

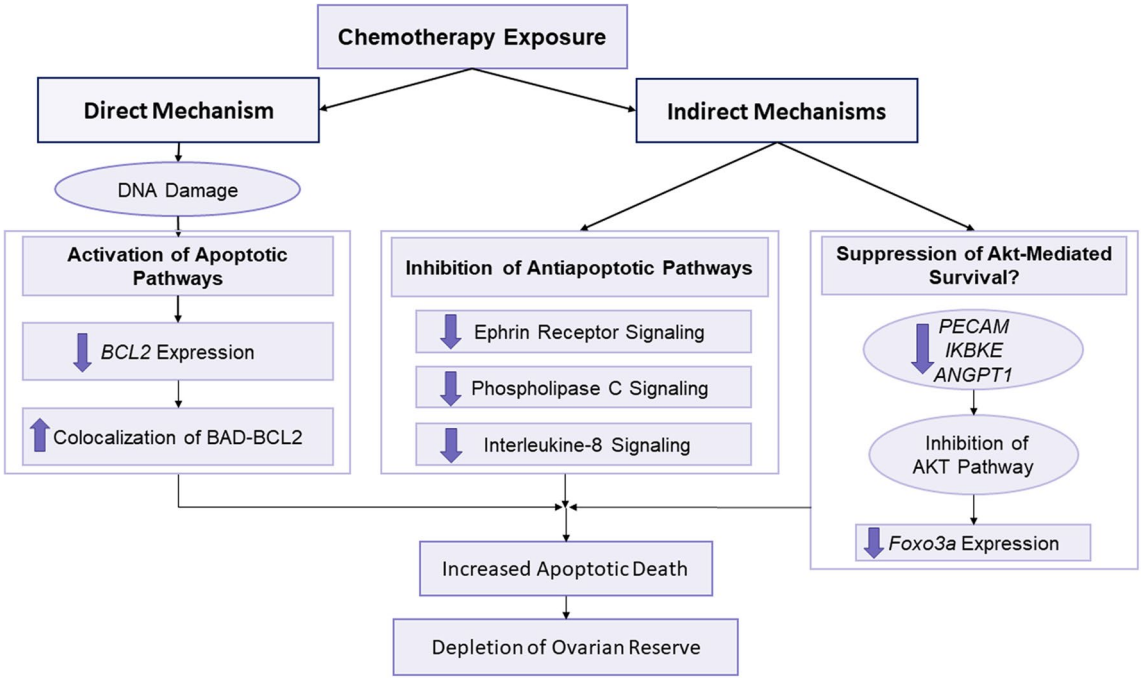


**Figure 6.** Mechanisms of acute chemotherapy-induced damage to ovarian reserve in human. Chemotherapy exposure induces apoptotic death in primordial follicles by direct and indirect mechanisms, and results in the massive depletion of human ovarian reserve. Directly, gonadotoxic chemotherapy agents such as cyclophosphamide induce double-strand DNA breaks in human primordial follicle oocytes which results in the activation of apoptotic cascades and increased co-localization of BAD-BCL2. Indirectly, same chemotherapy exposure also leads to suppression of anti-apoptotic pathways such as the Ephrin Receptor Signaling, Phospholipase C Signaling, and Interleukin-8 Signaling. Likewise, indirect suppression of pro-Akt pathways such as PECAM-1 (Platelet/Endothelial Cell Adhesion Molecule-1), IKBKE (inhibitor of nuclear factor kappa-B kinase subunit epsilon) and ANGPT1 (Angiopoietin-1) likely leads to the inhibition of the pro-survival functions of the Akt pathway. The sum of the latter two indirect mechanisms is increased sensitivity to apoptotic, gonadotoxic agents. While this scheme explains the mechanisms of acute primordial follicle losses after chemotherapy, there could be other direct and indirect mechanisms responsible for delayed losses, which are not studied here. For more detailed discussion and an expanded figure, please refer to Szymanska et al., 2020.

be studied. However, given the magnitude of acute damage from DNA damage and apoptotic death, we propose that the research for the development of targeted medical gonadal fertility preservation treatments should primarily focus on preventing DNA damage and/or chemo-induced pro-apoptotic state in primordial follicles.

Received: 25 June 2020; Accepted: 9 November 2020
Published online: 11 January 2021

## References

1. *Cancer facts and Figures 2019. Atlanta GA: 2019* (1975).
2. Oktay, K. *et al.* Fertility preservation in patients with cancer: ASCO clinical practice guideline update. *J. Clin. Oncol.* **36**, 1994–2001 (2018).
3. Soleimani, R., Heytens, E., Darzynkiewicz, Z. & Oktay, K. Mechanisms of chemotherapy-induced human ovarian aging: Double strand DNA breaks and microvascular compromise. *Aging (Albany NY)* **3**, 782–793 (2011).
4. Li, F. *et al.* Sphingosine-1-phosphate prevents chemotherapy-induced human primordial follicle death. *Hum. Reprod.* **29**, 107–113 (2014).
5. Oktem, O. & Oktay, K. A novel ovarian xenografting model to characterize the impact of chemotherapy agents on human primordial follicle reserve. *Cancer Res.* **67**, 10159–10162 (2007).
6. Meirow, D., Biederman, H., Anderson, R. A. & Wallace, W. H. B. Toxicity of chemotherapy and radiation on female reproduction. *Clin. Obstet. Gynecol.* **53**, 727–739 (2010).
7. Kalich-Philosoph, L. *et al.* Cyclophosphamide triggers follicle activation and "burnout "; AS101 prevents follicle loss and preserves fertility. *Sci. Transl. Med.* **5**, 185–262 (2013).
8. Szymanska, K. J., Tan, X. & Oktay, K. Unraveling the mechanisms of chemotherapy-induced damage to human primordial follicle reserve: Road to developing therapeutics for fertility preservation and reversing ovarian aging. *Mol. Hum. Reprod.* **26**, 553–566 (2020).
9. Oktay, K., Bedoschi, G., Pacheco, F., Turan, V. & Emirdar, V. First pregnancies, live birth, and in vitro fertilization outcomes after transplantation of frozen-banked ovarian tissue with a human extracellular matrix scaffold using robot-assisted minimally invasive surgery. *Am. J. Obstet. Gynecol.* **214**(94), e1-94.e9 (2016).
10. Oktay, K. & Karlikaya, G. Ovarian function after transplantation of frozen, banked autologous ovarian tissue. *N. Engl. J. Med.* **342**, 1919–1919 (2000).

11. Oktay, K., Schenken, R. S. & Nelson, J. F. Proliferating cell nuclear antigen marks the initiation of follicular growth in the rat. *Biol. Reprod.* **53**, 295–301 (1995).
12. Kitajima, M. *et al.* Enhanced follicular recruitment and atresia in cortex derived from ovaries with endometriomas. *Fertil. Steril.* **101**, 1031–1037 (2014).
13. Gougeon, A. & Chainy, G. B. N. Morphometric studies of small follicles in ovaries of women at different ages. *J. Reprod. Fertil.* **81**, 433–442 (1987).
14. Picelli, S. *et al.* Full-length RNA-seq from single cells using Smart-seq2. *Nat. Protoc.* **9**, 171–181 (2014).
15. Pertea, M., Kim, D., Pertea, G. M., Leek, J. T. & Salzberg, S. L. Transcript-level expression analysis of RNA-seq experiments with HISAT, StringTie and Ballgown. *Nat. Protoc.* **11**, 1650–1667 (2016).
16. Hochberg, Y. B. Y. Controlling the false discovery rate: A practical and powerful approach to multiple testing. *J. R. Stat. Soc. Ser. B* **57**, 289–300 (1995).
17. Oktay, K., Karlikaya, G., Akman, O., Ojakian, G. K. & Oktay, M. Interaction of extracellular matrix and activin-A in the initiation of follicle growth in the mouse ovary1. *Biol. Reprod.* **63**, 457–461 (2000).
18. Limaye, V. *et al.* Sphingosine kinase-1 enhances endothelial cell survival through a PECAM-1-dependent activation of PI-3K/Akt and regulation of Bcl-2 family members. *Blood* **105**, 3169–3177 (2005).
19. Fleming, I., Fisslthaler, B., Dixit, M. & Busse, R. Role of PECAM-1 in the shear-stress-induced activation of Akt and the endothelial nitric oxide synthase (eNOS) in endothelial cells. *J. Cell Sci.* **118**, 4103–4111 (2005).
20. Xie, X. *et al.* IkappaB kinase epsilon and TANK-binding kinase 1 activate AKT by direct phosphorylation. *Proc. Natl. Acad. Sci. U. S. A.* **108**, 6474–6479 (2011).
21. Mahajan, K. & Mahajan, N. P. PI3K-independent AKT activation in cancers: A treasure trove for novel therapeutics. *J. Cell. Physiol.* **227**, 3178–3184 (2012).
22. Papapetropoulos, A. *et al.* Angiopoietin-1 inhibits endothelial cell apoptosis via the Akt/survivin pathway. *J. Biol. Chem.* **275**, 9102–9105 (2000).
23. Campbell, K. J. & Tait, S. W. G. Targeting BCL-2 regulated apoptosis in cancer. *Open Biol.* **8**, 2 (2018).
24. Zinkel, S., Gross, A. & Yang, E. BCL2 family in DNA damage and cell cycle control. *Cell. Death Differ.* **13**, 1351–1359 (2006).
25. Susnow, N., Zeng, L., Margineantu, D. & Hockenbery, D. M. Bcl-2 family proteins as regulators of oxidative stress. *Semin. Cancer Biol.* **19**, 42–49 (2009).
26. Pihán, P., Carreras-Sureda, A. & Hetz, C. BCL-2 family: Integrating stress responses at the ER to control cell demise. *Cell. Death Differ.* **24**, 1478–1487 (2017).
27. Roufayel, R. Regulation of stressed-induced cell death by the Bcl-2 family of apoptotic proteins. *Mol. Membr. Biol.* **33**, 89–99 (2016).
28. Wang, H. G. *et al.* $Ca^{2+}$-induced apoptosis through calcineurin dephosphorylation of BAD. *Science (80-).* **284**, 339–343 (1999).
29. Liu, J., Li, M., Zeng, W.-S., Bai, X.-C. & Luo, S.-Q. Inhibition of phospholipase C gamma1 signaling pathway promotes apoptosis of human colorectal carcinoma cells. *Di Yi Jun Yi Da Xue Xue Bao* **25**, 177–180 (2005).
30. Maddigan, A. *et al.* EphB receptors trigger Akt activation and suppress fas receptor-induced apoptosis in malignant T lymphocytes. *J. Immunol.* **187**, 5983–5994 (2011).
31. Stronach, E. A. *et al.* The role of interleukin-8 (IL-8) and IL-8 receptors in platinum response in high grade serous ovarian carcinoma. *Oncotarget* **6**, 31593–31603 (2015).
32. Heckman, C. A., Mehew, J. W. & Boxer, L. M. NF-κB activates Bcl-2 expression in t(14;18) lymphoma cells. *Oncogene* **21**, 3898–3908 (2002).
33. John, G. B., Gallardo, T. D., Shirley, L. J. & Castrillon, D. H. Foxo3 is a PI3K-dependent molecular switch controlling the initiation of oocyte growth. *Dev. Biol.* **321**, 197–204 (2008).
34. Wandji, S.-A., Sršeň, V., Voss, A. K., Eppig, J. J. & Fortune, J. E. Initiation in vitro of growth of bovine primordial follicles1. *Biol. Reprod.* **55**, 942–948 (1996).
35. Luo, Q. *et al.* Role of SDF-1/CXCR4 and cytokines in the development of ovary injury in chemotherapy drug induced premature ovarian failure mice. *Life Sci.* **179**, 103–109 (2017).
36. Luan, Y., Edmonds, M. E., Woodruff, T. K. & Kim, S. Y. Inhibitors of apoptosis protect the ovarian reserve from cyclophosphamide. *J. Endocrinol.* **240**, 243–256 (2019).
37. Nguyen, Q. N. *et al.* Cisplatin- and cyclophosphamide-induced primordial follicle depletion is caused by direct damage to oocytes. *MHR Basic Sci. Reprod. Med.* https://doi.org/10.1093/molehr/gaz020 (2019).
38. Perez, G. I., Knudson, C. M., Leykin, L., Korsmeyer, S. J. & Tilly, J. L. Apoptosis-associated signaling pathways are required for chemotherapy-mediated female germ cell destruction. *Nat. Med.* **3**, 1228–1232 (1997).
39. Hata, A. N., Engelman, J. A. & Faber, A. C. The BCL2 family: Key mediators of the apoptotic response to targeted anticancer therapeutics. *Cancer Discov.* **5**, 475–487 (2015).
40. Gao, C. *et al.* PECAM-1 functions as a specific and potent inhibitor of mitochondrial-dependent apoptosis. *Blood* **102**, 169–179 (2003).
41. Parborell, F., Abramovich, D., Irusta, G. & Tesone, M. Angiopoietin 1 reduces rat follicular atresia mediated by apoptosis through the PI3K/Akt pathway. *Mol. Cell. Endocrinol.* **343**, 79–87 (2011).


## Acknowledgements

We would like to acknowledge LiveonNY for their assistance in locating organ donors and obtaining whole ovaries for this research project. We thank the Yale Center for Advanced Light Microscopy Facility for their assistance with their microscopy service. The Leica SP8 Gated STED 3X super resolution microscope was funded by shared instrument Grant # NIH S10 OD020142.

## Author contributions

K.O. designed the study and conceived the idea, S.T., B.M., V.T., E.T., K.S. performed the experiments, S.T. and K.S. analyzed the results, R.G. assisted with bioinformatic analysis, K.O., S.T., and K.S. wrote the manuscript.

## Funding

Research was supported by R01 HD053112 from the *Eunice Kennedy Shriver* National Institute of Child Health and Human Development of the National Institutes of Health.

## Competing interests

The authors declare no competing interests.

## Additional information

**Supplementary Information** The online version contains supplementary material available at https://doi.

org/10.1038/s41598-020-79643-x.

**Correspondence** and requests for materials should be addressed to K.O.